Carbohydrate Polymers 117 (2015) 54–62

Contents lists available at ScienceDirect

Carbohydrate Polymers

journal homepage: www.elsevier.com/locate/carbpol

Preparation, characterization and *in vitro* digestibility of gellan and chitosan–gellan microgels

Joice Aline Pires Vilela, Fabiana de Assis Perrechil, Carolina Siqueira Franco Picone, Ana Carla Kawazoe Sato, Rosiane Lopes da Cunha *

Department of Food Engineering, School of Food Engineering, University of Campinas (UNICAMP), R. Monteiro Lobato, 80, 13083-862 Campinas, SP, Brazil

ARTICLE INFO

Article history:
Received 31 January 2014
Received in revised form 18 August 2014
Accepted 11 September 2014
Available online 26 September 2014

Keywords:
Microgel
Gellan
Chitosan
In vitro digestion

ABSTRACT

Gellan microgels with potential application in delivery systems were obtained by physically cross-linked gellan gum. The microgels were produced by atomization followed by ionotropic gelation using $CaCl_2$ (gellan/Ca) or KCl (gellan/K) as hardening agent and part of them were coated with chitosan in order to improve their resistance to gastric digestion. Size distribution, morphology and zeta potential of microgels were evaluated before and after *in vitro* digestion process. The long term stability was also evaluated. Spherical microparticles were obtained at gellan concentration above 0.6% w/w, showing average size among 70–120 μm. Most of the coated and uncoated microgels showed stability in aqueous media, except the uncoated gellan/K microgel. The *in vitro* digestion evaluation showed that all particles maintained their size and shape after the gastric digestion step. However, the enteric digestion caused disintegration of microgels indicating their potential application for enteric delivery systems. The chitosan-coated microgels showed lower degree of fragmentation when compared to the uncoated microgels, indicating that the coating process enable a better control of microgels releasing properties during the enteric digestion.

1. Introduction

Microgels are gel particles of micrometric dimensions (Oh, Lee, & Park, 2009) which present several applications as encapsulation matrix of bioactive compounds as well as texture modifier agents. Microgels based on biopolymers such as polysaccharides can be added to food, cosmetics and pharmaceutical products without risk to health, since most of these compounds are nontoxic and biocompatible. Polysaccharides microgels can be formed by physical cross-linking, in which hydrophobic and electrostatic interactions are mainly involved in the gel network formation (Das, Zhang, & Kumacheva, 2006). The greater advantage offered by microgels is their flexibility, since the final properties as well as their response to the environmental conditions can be easily tuned.

Microgels properties depend on their composition and the process conditions selected for their manufacturing. Several methods can be used to produce microgels (Poncelet et al., 1992; Das et al., 2006; Herrero, Del-Valle, & Galán, 2006; Li, Rouaud, & Poncelet, 2008; Perrechil, Sato, & Cunha, 2011; Perrechil, Vilela, Guerreiro, & Cunha, 2012). For biopolymer-based microgels, emulsification and extrusion processes are the most used for droplets formation before the gelation step. Among the extrusion-based methods, the atomization process allows the production of micrometer size droplets through a simple apparatus and without the use of drastic process conditions such as intensive heating or organic solvents. The droplets are collected in a bath containing gelling agents, like salts, that can diffuse into the polysaccharide droplets to form the microgels (Herrero et al., 2006; Perrechil et al., 2011).

The gellan gum is a negatively charged polysaccharide produced by the microorganism *Sphingomonas elodea*. Gellan is composed of repeating tetrasaccharide (1,3-β-D-glucose, 1,4-β-D-glucuronic acid, 1,4-β-D-glucose, 1,4-α-L-rhamnose) units containing one carboxyl side group (Jansson & Lindberg, 1983). It has the ability to form gel by the addition of salts or acids, and the gelation can occur even at low gellan concentration. The gelation occurs in two steps: first there is the formation of double helices during cooling, followed by the cation-mediated aggregation of the double helices leading to gelation (Miyoshi, Takaya, & Nishinari, 1996). The bulk gels of gellan have been widely studied and a wide variety of textures/mechanical properties is found depending on the gelation conditions (Sworn, Sanderson, & Gibson, 1995; Tang, Tung, & Zeng, 1996; Yamamoto & Cunha, 2007; Evageliou, Karantoni, Mandala, & Komaitis, 2010; Vilela, Cavallieri, & Cunha, 2011; Picone & Cunha, 2011; Norton, Cox, & Spyropoulos, 2011). Gellan gum can also form

* Corresponding author. Tel.: +55 19 3521 4047; fax: +55 19 3521 4027.
E-mail address: rosiane@fea.unicamp.br (R.L.d. Cunha).

http://dx.doi.org/10.1016/j.carbpol.2014.09.019
0144-8617/

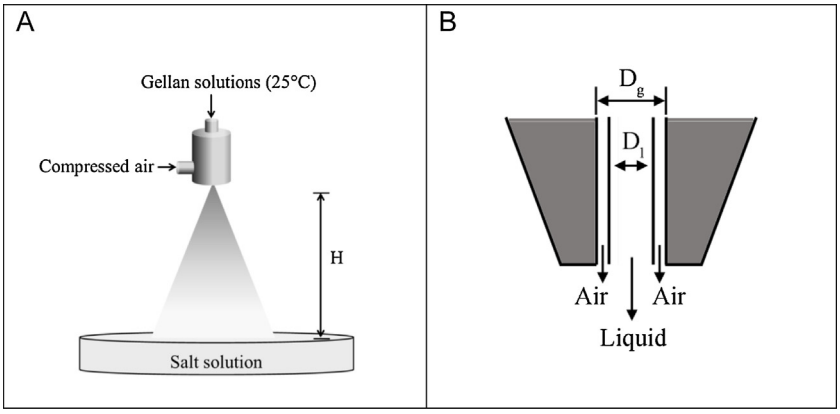

Fig. 1. (A) Extrusion for microgels formation and (B) Atomizer nozzle. H = height from the atomizer nozzle to the salt solution, D_l = diameter of the fluid nozzle exit and D_g = diameter of gas nozzle exit (Adapted from Perrechil et al., 2011).

polyelectrolyte complexes with oppositely charged polymers such as chitosan (Amaike, Senoo, & Yamamoto, 1998; Ohkawa, Kitagawa, & Yamamoto, 2004).

Chitosan is a positively charged polysaccharide obtained by the alkaline deacetylation of the chitin. The chitosan structure is composed by units of *N*-acetyl-2-amino-2-deoxy-D-glucopyranose and 2-amino-2-deoxy-D-glucopyranose linked by (1 → 4)-β-glycosidic bonds (Dash, Chiellini, Ottenbrite, & Chiellini, 2011). Particles coated with chitosan show enhanced protective capacity (Zou et al., 2011; Colinet, Dulong, Mocanu, Picton, & Cerf, 2010; Cook, Tzortzis, Charalampopoulos, & Khutoryanskiy, 2011) and notably increase their mucoadhesion properties, since the mucus layer of the gastrointestinal tract show negative charge (Allen, Flemström, Garner, & Kivilaakso, 1993). The mucoadhesion is a relevant property for encapsulation matrix, because it is related to the residence time of the particles in the gastrointestinal tract (Gåserød, Jolliffe, Hampson, Dettmar, & Skjåk-Bræk, 1998; Harding, 2003) and to the absorption rate of the bioactive compound.

Therefore, the purpose of this study was to investigate the potential as encapsulating matrix of the gellan microgels produced by atomization followed by ionotropic gelation using mono (K^+) or divalent (Ca^{2+}) cations as gelation agents. The effect of the chitosan coating on the particles properties and stability was also studied.

2. Material and methods

2.1. Materials

Deacylated gellan gum (Kelcogel) was kindly donated by Kelco Biopolymers (San Diego, CA) and it was used without further purification. Chitosan (deacetylation degree ~86%) was purchased from Primex Ingredients SA (Iceland). The other reagents were of analytical grade and purchased from Sigma-Aldrich Corporation (St. Louis, USA).

2.2. Preparation of biopolymers solutions

Gellan solutions were prepared by the dispersion of the powder in deionized water, followed by heat treatment at 70 °C for 30 min under magnetic stirring. After that, these solutions were cooled to 25 °C using a water bath. The chitosan solution (0.25% w/w) was obtained by dissolving the polysaccharide in sodium acetate buffer 0.2 M (pH = 3.0 ± 0.1) under magnetic stirring at room temperature for 12 h.

2.3. Gellan microgels production

The extrusion process used for the microgels production was adapted from the Perrechil et al. (2011). The gellan solutions (25 °C) at different concentration (0.4, 0.6, 0.8, 1 and 1.2% w/w) were extruded by an atomizer nozzle (D_l = 0.7 mm and D_g = 2.5 mm) into KCl or $CaCl_2$ solutions to produce the microgels. The height from the atomizer nozzle to the salt solutions (Fig. 1) was H = 200 mm, the feed flow rate was 0.18 L/h and the compressed air (absolute pressure of 200 kPa) flow rate at the nozzle was 1628 L/h (~150 m/s). The extruded particles were maintained in the salt solution under magnetic stirring for 30 min and then filtered through a sieve with opening of 0.037 mm. The concentration of salt solutions was 2.28% (w/v) KCl or 1.1% (w/v) $CaCl_2$, which resulted in the same ionic strength (0.3 M). Morphology, particle size distribution and zeta potential of these microgels were evaluated, as well as their long term stability.

2.4. Chitosan coating

Gellan microgels (0.6, 0.8, 1 and 1.2% w/w) formed by ionic gelation with $CaCl_2$ (gellan/Ca) or KCl (gellan/K) were dispersed into a solution of chitosan under magnetic stirring for 30 min. The addition of the microgels into the solution of chitosan was done in two steps to prevent the formation of agglomerates. First, the gellan particles were dispersed in sodium acetate buffer 0.2 M (pH 3.0) and then, chitosan solution (0.5% w/w) was added gradually, resulting in a final dispersion containing 20% w/w of particles in 0.25% (w/w) chitosan solution. The dispersions were filtered through a sieve opening of 0.037 mm, and the morphology, particle size distribution and zeta potential of these microgels (gellan/Ca/chitosan and gellan/K/chitosan) were evaluated. The long term stability of these microgels was also determined in order to compare with uncovered microgels.

2.5. Stability

To check for microparticle stability, suspensions were prepared by dispersing 10% (w/w) microgels (1% w/w gellan) in distilled water or in sodium acetate buffer 0.2 M (pH 3). These microgel suspensions were stored at 10 °C and fractions were collected to evaluate their mean size, D_{32} (Section 2.7.1), during 15 days. The stability evaluation was done considering the ratio between the mean size measured at final time (D) to the initial mean size (D_0).

2.6. In vitro digestion

The microgels (1% w/w gellan) were added to phosphate buffer (0.005 M, pH 6.9, 1 M NaCl + 0.004 M $CaCl_2$) at a ratio of 1 g of each sample to 4 mL of buffer (Hoebler et al., 2002). The gastric digestion was simulated by the addition of a gastric juice composed of porcine pepsin (40 mg/mL in 0.1 M HCl) to the initial mixtures, which was added at a ratio of 0.5 g of pepsin per 100 g of sample (Miller, Schricker, Rasmussen, & Van Campen, 1981; Garrett, Failla, & Sarama, 1999). The pH was adjusted to 2 by adding HCl (6 M), and then this mixture was incubated for 1 h at 37 °C under orbital stirring. For the enteric digestion, the resulting mixtures were neutralized to pH 5.3 using sodium bicarbonate solution 0.9 M, then a mixture of pancreatin and bile extract (2 mg/mL pancreatin + 12 mg/mL porcine bile extract) was added. The pH of the mixture was adjusted to 7 prior to its incubation at 37 °C for 2 h under orbital stirring. The morphology, particle size distribution and zeta potential of the particles were evaluated after the gastric and enteric digestion steps. For the zeta potential, aliquots of the incubated mixtures were collected and diluted in distilled water before the measurement.

2.7. Microgels evaluation

2.7.1. Size distribution and mean diameter

The particles size distribution was determined by laser diffraction technique using a Mastersizer 2000 (Malvern Instruments Ltd., UK). All measurements were performed in triplicate. The average particle size was determined from the Sauter mean diameter (D_{32}), which is defined as the diameter of the sphere with the same volume/surface area of the particle (Eq. (1)).

$$D_{32} = \frac{\sum n_i d_i^3}{\sum n_i d_i^2} \quad (1)$$

where n_i is the number of particles with diameter d_i.

2.7.2. Optical microscopy

Microgels morphology was evaluated by optical microscopy using a Scope A1 microscope (Carl Zeiss, Germany) with a 10× objective lens. The particles were poured onto microscope slides and carefully covered with glass cover slips. At least 20 images were obtained for each sample. The gellan microgels were stained with methylene blue, and the chitosan–gellan microgels were stained with Congo Red dye.

2.7.3. Confocal scanning laser microscopy (CSLM)

Fluorescein-5-isothiocyanate (FITC) was used for the covalent labeling of gellan, following the method described by Heilig, Göggerle, and Hinrichs (2009). 20 mL dimethyl sulfoxide (DMSO) and 80 μL pyridine were mixed with 1 g gellan and stirred at room temperature for 30 min. After the addition of 0.1 g FITC and 40 μL dibutyltin dilaurate, the mixture was incubated for 3 h in a 95 °C water bath and, finally, cooled down to room temperature. The resulting gel was then minced, washed with ethanol 99.6% and dried at 65 °C. The covalently labeled gellan powder was dissolved and used to prepare the polysaccharide solution. Chitosan solution was stained using a fluorescent dye Rhodamine B. Each labeled solution was then used to prepare the uncoated and coated microgels as previously described. Samples were examined using a Zeiss LSM 780-NLO confocal on an Axio Observer Z.1 microscope (Carl Zeiss AG, Germany) with a 10 × objective. Images were collected using 488 and 543 nm laser lines for excitation of FITC and Rhodamine B fluorophores, respectively.

2.7.4. Zeta potential

Zeta potential was determined by Dynamic Light Scattering using a Nanosizer Zeta ZS (Malvern Instruments LTD., UK) with a detection angle of 173°. The zeta potential was estimated from the electrophoretic mobility measurements using the Smoluchowski model. The zeta potential of pure polysaccharides was measured using dispersions (0.1% w/w) in deionized water and in sodium acetate buffer (pH = 3) for the gellan and chitosan, respectively. The zeta potential of the microgels was measured using a microgel suspension in distilled water containing 1% (w/w) of particles. This concentration was necessary to obtain proper quality of results and it was determined through preliminary tests. All measurements were performed in triplicate.

2.8. Statistical analyses

Significant differences ($p < 0.05$) between microgel properties were determined by a one-way analysis of variance, and the comparison between the mean values was evaluated by the Tukey procedure. The statistical analyses were performed using the software STATISTICA 7 (Statisoft Inc., Tulsa, USA).

3. Results and discussion

3.1. Microgel morphology

Fig. 2 shows the morphology of gellan/Ca (A–E) and gellan/K microgels (G–K) at different polysaccharide concentrations. The gelling agent (hardening) was added to the gellan droplets after the coil-helix transition, *i.e.*, after the heat treatment in the cooled solution at 25 °C. The coil-helix conformational transition occurred during the cooling of the gellan solution at temperatures around 30 °C (Picone & Cunha, 2011). In most studies concerning gellan macrogels, gelling agents (salts or acids) are added to the hot solution, i.e., to the coil gellan solution (Tang et al., 1996; Mao, Tang, & Swanson, 1999; Evageliou et al., 2010; Picone & Cunha, 2011). This procedure allows the complete mixture of the system (gellan and gelling agents) before the macrogel formation, which occurs when the system crosses through the transition or sol-gel temperature. The direct addition of gelling agents to a solution of helices (cold gelation) results in inhomogeneous macrogels, since gelation occurs instantaneously, hindering the dispersion of the gelling agents throughout the solution. Using a dialysis membrane that allows the slow diffusion of salts into the gellan solution can resolve such limitation, making possible the cold gelation of gellan macrogels (Vilela et al., 2011). However, the cold-set gelation of microparticles was possible because of their small size resulting in a high surface area/volume ratio. Therefore a great exposure of the helix occurs, allowing a fast diffusion of the gelling agents and the formation of a gel network.

Microparticles composed by the lower concentration of gellan (0.4% w/w) showed filaments and irregularly shaped structures, with no spherical particles (Fig. 2A and G). These structures disintegrated in few minutes after extrusion probably because the weaker gel formed did not resist to mixing and flow. The formation of microgels was observed at gellan concentrations higher than 0.6% w/w and the increase of the polysaccharide concentration led to more spherical gels. The gellan gum has the ability to form gels at considerably low concentration of polysaccharide and gelling agents in comparison with other gelling polysaccharides, as κ-carrageenan (Perrechil et al., 2011) and alginate (Chan, Lee, Ravindra, & Poncelet, 2009). Concerning to the hardening agent, more spherical gellan/Ca particles were achieved at lower polysaccharide concentration in comparison with gellan/K particles. Even though both salt solutions showed the same ionic strength, the

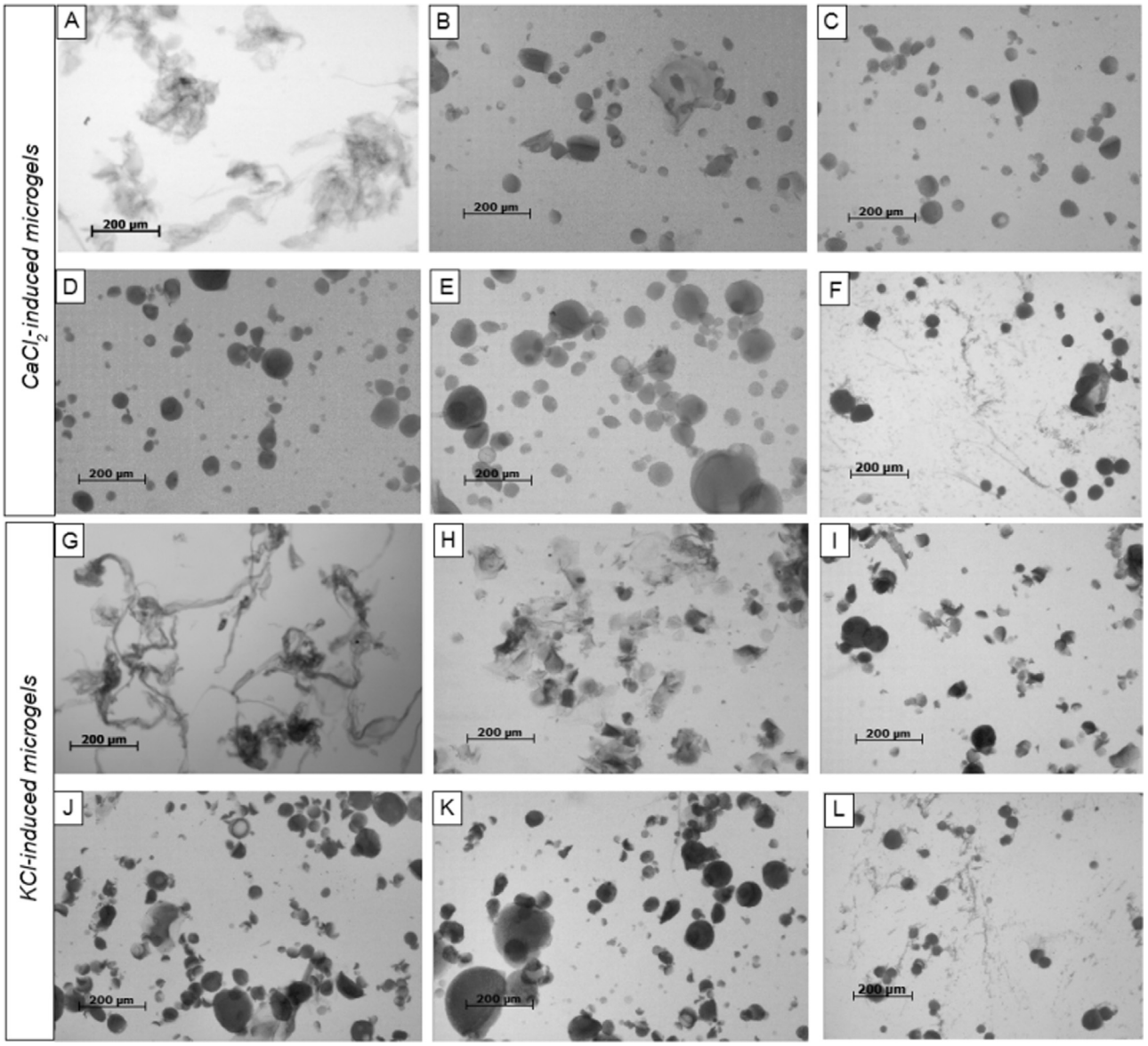

Fig. 2. Optical microscopy (10× magnification). Microgels with gelation induced by $CaCl_2$ with (A) 0.4, (B) 0.6, (C) 0.8, (D) 1 and (E) 1.2% (w/w) of gellan concentration. (F) 1% (w/w) gellan/Ca microgel coated with chitosan. Microgels with gelation induced by KCl with (G) 0.4, (H) 0.6, (I) 0.8, (J) 1 and (K) 1.2% (w/w) of gellan concentration. (L) 1% (w/w) gellan/K microgel coated with chitosan. The bars represent 200 μm.

type of interaction promoted by salts with different valences is not the same (Morris, Nishinari, & Rinaudo, 2012). Monovalent cations promote indirect crosslinking in the double helices, forming linkages by shielding the electrostatic repulsion of the carboxylate groups, while divalent cations can establish direct interaction between the carboxylate groups of adjacent double helices being more effectiveness in gel formation (Tang et al., 1996). Previously researches have showed that even using the same ionic strength of salt solutions, the gel hardness is higher with divalent cations (Tang et al., 1996; Vilela et al., 2011). Such results could explain the more fragmented structures observed in gellan/K microgels, since a weaker gel network is obtained under this condition.

Fig. 2F and L shows the gellan/Ca and gellan/K microgels coated with chitosan. The shape of the microgels was similar in both systems, but the filaments observed could be related to an excess of chitosan that did not associate to the gellan particles.

3.2. Mean size

Fig. 3A and B shows the particle size distribution of gellan/Ca and gellan/K microgels. In general, the increase of gellan concentration shifted the particle size distribution toward larger particles size. Since the same process conditions were used in the extrusion of all solutions, such behavior could be attributed to the higher viscosity of the dispersion with increased gellan concentration. Viscous solutions are known to form larger particles during the extrusion process, since the disintegration of the bulk solution in droplets becomes more difficult with the increase in the viscosity (Herrero et al., 2006). However the gellan dispersions showed shear thinning behavior (data not shown), showing a decrease of the viscosity as the shear rate increase. During the extrusion process the shear rate applied to the solutions at the droplets formation was considerably high, reaching values close to 7000 s^{-1} (estimated by the ratio between gas velocity and nozzle diameter). The estimated

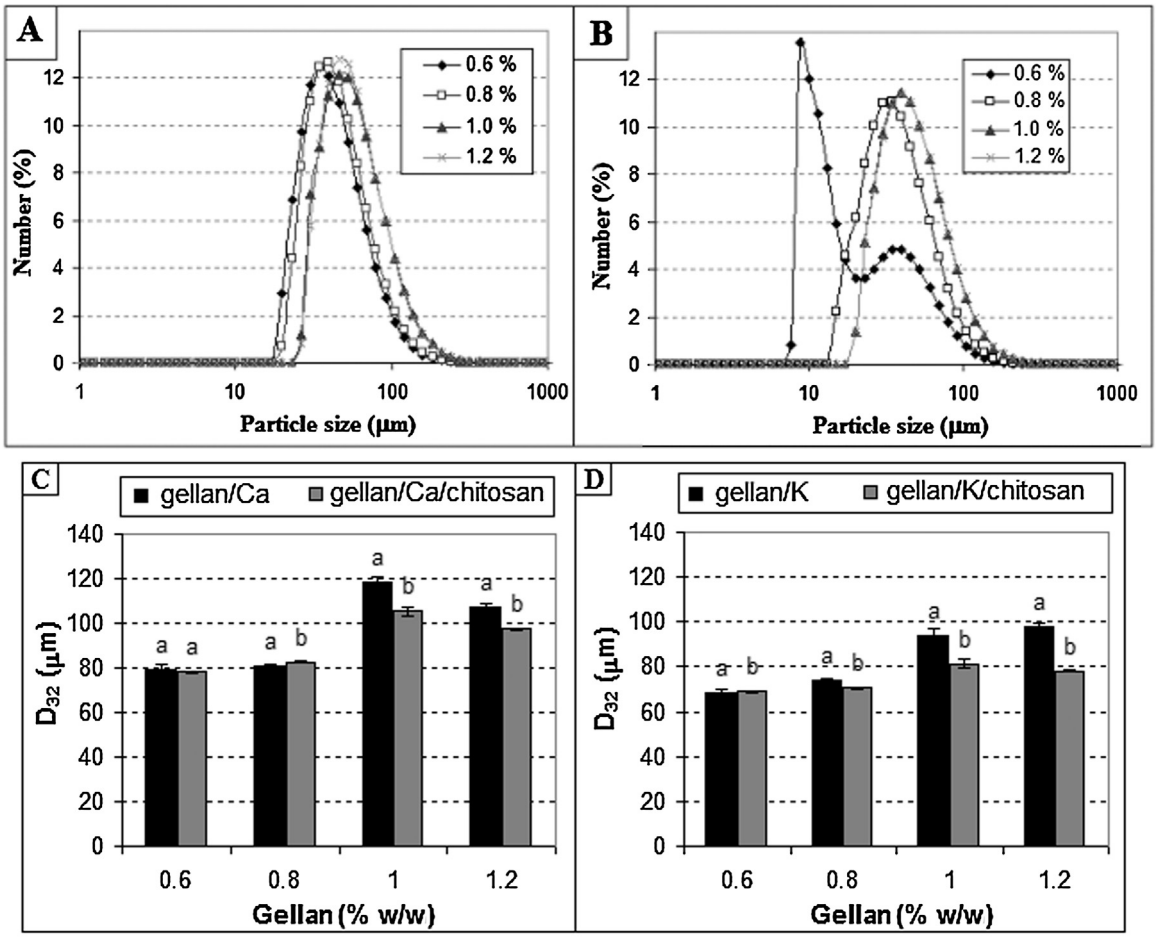

Fig. 3. Particle size distribution curves of the gellan microgels induced by $CaCl_2$ (A) or KCl (B). Mean size (D_{32}) of the gellan microgels induced by $CaCl_2$ (C) or KCl (D) before and after the chitosan coating. Different letters show the differences amongst the same gellan concentration with or without the chitosan layer.

viscosity at this shear rate varies between 9 and 16 mPa for the different gellan solutions studied. Compared to the viscosity at a shear rate of 50 s^{-1}, in which values between 9 and 650 mPa were observed, the difference between viscosity values during extrusion process is smaller, but it could be considered significant. Moreover, right after the extrusion process the shear rate begin to decrease substantially and at the moment that the particles reach the hardening bath, the shear rate could be quite low. In this step viscosity can play a major role and it can be the main factor influencing the gelation process, the morphology and size of the produced particles.

Concerning the gelation step with the different salts, the gellan/K microgels showed a great amount of smaller particles than the gellan/Ca microgels, which was clearer for the gellan/K microgels with the lowest gellan concentration (0.6% w/w). This system showed a bimodal distribution curve, which can be related to the breaking of these weaker microgels during the homogenization process (hardening). Such fragile structure could be a result of the use of monovalent salts combined with the smaller polysaccharide concentration (Tang et al., 1996; Vilela et al., 2011).

The changes in microgels size after the chitosan coating was dependent on the initial gellan concentration (Fig. 3C and D). Microgels at lower gellan concentration (0.6 and 0.8% w/w) showed no significant changes in particle size, independent of the salt used for gelation. On the other hand, microgels at higher gellan concentration showed a decrease in particle size. Ribeiro, Neufeld, Arnaud, and Chaumeil (1999) observed that the size change after chitosan coating was dependent on the chitosan molecular weight and the coating time. A decrease of particles size was observed only for the coating with the low molecular weight chitosan. Deacetylation degree is another chitosan property that influences the complex formed, since it exerts influence on the charge density determining the amount of chitosan attached to the anionic microparticle surface (Kiang, Wen, Lim, & Leong, 2004). However in our work the chitosan molecular weight and deacetylation degree were the same in all samples and the difference observed could be related to the gellan/chitosan ratio, since the formation of polyelectrolyte complexes is affected by the systems composition. We assumed that the size decrease could be associated to the electrostatic interactions between the polysaccharides (oppositely charged), promoting particles compaction with water loss and consequently changing the particles structure and size.

3.3. Zeta potential

Fig. 4A shows zeta potential of the gellan/K and gellan/Ca microgels before and after the chitosan coating. The zeta potential of pure gellan dispersed in water was -44.27 ± 3.71 mV and after the formation of the gellan-salts microgels the gellan/Ca particles showed negative zeta potential values around −12 mV, while zeta potential of gellan/K particles was around −17 mV. These results suggest that screening charge performed by calcium was higher, which can be related to the higher effectiveness of divalent cations in the formation of gellan gels (Tang et al., 1996). The polysaccharide concentration did not significantly affect the zeta potential of microgels. This result showed that the salt concentrations used were in excess in both cases, with KCl or $CaCl_2$.

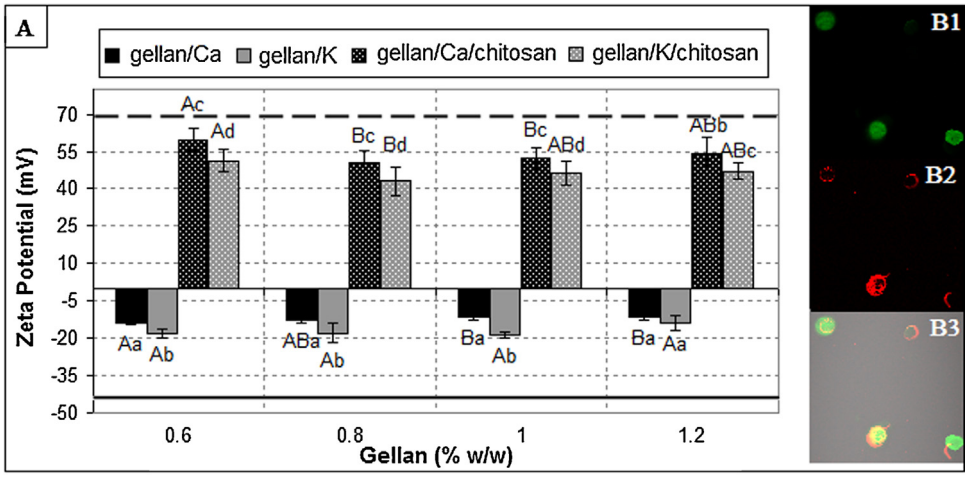

Fig. 4. (A) Zeta potential of the gellan microgels with gelation induced by $CaCl_2$ (gellan/Ca) or KCl (gellan/K) before and after the chitosan coating (gellan/Ca/chitosan or gellan/K/chitosan). Pure chitosan (— —) and pure gellan (—). Capital letters show the differences amongst the formulations with different gellan concentration. Small letters show the differences amongst differents formulations made with the same gellan concentration. (B) Confocal microscopy of gellan/Ca/chitosan microgels: (B1) FTIC-labeled gellan, (B2) rhodamine-labeled chitosan and (B3) Merged image of (B1) and (B2).

The positive zeta potential values of microgels after coating with chitosan confirmed that indeed the particles were recovered. The zeta potential of pure chitosan dispersed in sodium acetate buffer (pH = 3) was also determined, and showed a value of +69.07 ± 2.13 mV. Anal, Tobiassen, Flanagan, and Singh (2008) reported that zeta potential values of chitosan solutions were strongly positive between pH 3.0 and 5.5, with almost constant value around +52 mV. Zhang and Kosaraju (2007) showed that the zeta potential of pure chitosan at pH 3.0 was +56.1 mV. The difference among the values could be attributed to minor differences in the dispersant media, molecular weight and deacetylation degree of the chitosan or even the presence of small amount of impurities in solution (Delgado, Gonzalez-Caballero, Hunter, Koopal, & Lyklema, 2005). All chitosan-coated microgels showed lower zeta potential values than pure chitosan dispersion, which also confirms the polyelectrolyte complex formation. Fig. 4B shows the confocal microscopy of gellan/Ca microgels. The gellan is green (Fig. 4B1) and chitosan is red (Fig. 4B2). The Z-scanning showed "solid" spherical gellan particles covered by a thin chitosan layer. The overlapping of both images suggests that gellan forms the particle core while chitosan is covering it (Fig. 4B3), as expected according to the layer-by-layer approach (Guzey & McClements, 2006; Yang, Xia, Tan, & Zhang, 2013; Luo & Wang, 2014). As observed for the uncovered particles, gellan concentration did not affect the zeta potential of the coated microgels. The gellan/Ca particles showed higher zeta potential values after coating than gellan/K for all gellan concentrations. This result is corroborated by the charge balance, since the same amount of chitosan was used to coat both particles. Thus the particle with higher negative value before coating became the particle with lower positive value after coating. Although the same chitosan content was used to coat all particles, we cannot guarantee that the same amount of chitosan was attached per area of surface. However, it seems that the amount of chitosan used was in excess and all samples achieved an equilibrium state.

3.4. Stability

Particles stability in aqueous systems at different pH values was evaluated from the variation of mean diameter ratio (D/D_0) during 15 days of storage. This period of storage seems to be enough for some applications in food or pharmaceutical products with high water content. Table 1 shows the microgels stability in water (pH ~ 6.3) and in sodium acetate buffer (pH ~ 3).

In general, microgels size remained almost unchanged during the 15 days of storage except the uncoated gellan/K, which quickly dissolved when added to distilled water. Probably the interaction between the gellan chains and this monovalent cation were not strong enough to prevent the salt diffusion to the water, leading to gel network disruption. On the other hand, the gellan/K microgels remained stable in sodium acetate buffer. The amount of H^+ ions present at this low pH solution prevented the gel network destabilization, either by avoiding the salt migration to the solution due to a osmotic equilibrium or even by the diffusion of H^+ ions into the gel network, reinforcing it. Nitta, Ikeda, and Nishinari (2006) reported an enhancement of gellan gel rigidity through immersion of macrogels in solutions containing monovalent cations, an evidence of these ions diffusion into the gel network and their positive effect in the stability of the gels. The H^+ ions of the acidic solution could show a similar effect that was observed in the presence of monovalent cations of salts.

The coated microgels also showed good stability in both dispersant. It is interesting to notice that even the KCl-induced microgel remained stable in distilled water after the chitosan coating. It seems that the external layer of chitosan avoids the potassium

Table 1
Microgels stability at different pH values.

	Distilled water				Sodium acetate buffer			
	D/D_0				D/D_0			
Time (days)	0	6	10	15	0	6	10	15
Gellan/Ca	1^{A}	1.00^{A}	0.98^{B}	0.99^{AB}	1^{A}	0.94^{B}	0.92^{B}	0.94^{B}
Gellan/K	–	–	–	–	1^{A}	1.00^{A}	0.98^{A}	0.91^{A}
Gellan/Ca/chitosan	1^{A}	0.98^{A}	0.96^{A}	0.99^{A}	1^{A}	1.20^{B}	1.05^{A}	1.02^{A}
Gellan/K/chitosan	1^{A}	1.05^{A}	1.00^{A}	0.99^{A}	1^{A}	1.06^{B}	1.04^{AB}	0.99^{A}

Different letters indicate significant differences at $p < 0.05$ in the same sample/buffer system.

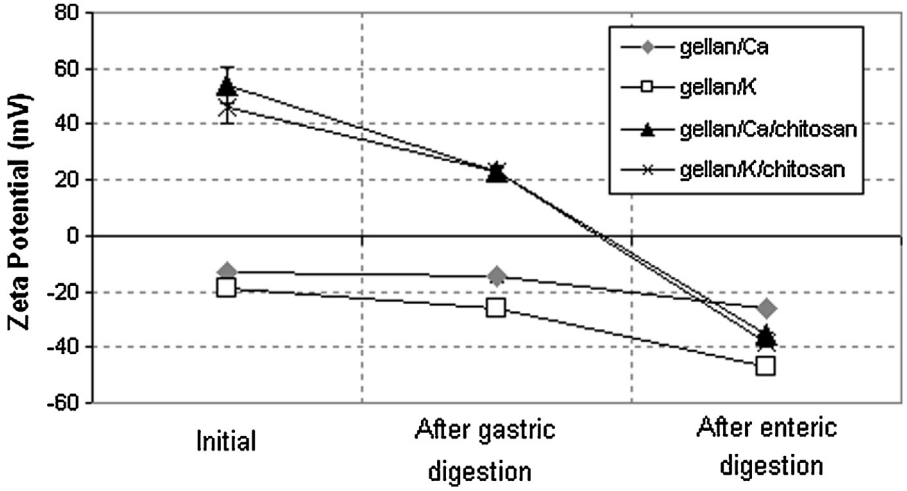

Fig. 5. Effect of digestion steps on the zeta potential of microgels induced by $CaCl_2$ (gellan/Ca) or KCl (gellan/K), with or without chitosan coating (gellan/Ca/chitosan and gellan/K/chitosan).

migration to the water or this salt became unnecessary or less relevant to maintain the gel network after the polyelectrolyte complex formation between gellan and chitosan. The stability of polyelectrolyte complex is dependent on the polysaccharides charge density, which can result in attractive or repulsive interactions depending on the medium conditions (Hamman, 2010). The medium pH used in this work (pH ~ 6.3 or pH ~ 3) apparently did not affect the polyelectrolyte interactions keeping the complex intact.

3.5. *In vitro digestion*

The gellan microgels induced by $CaCl_2$ or KCl, with or without coating of chitosan were subjected to *in vitro* digestion. Microgels properties (zeta potential and particle size distribution and morphology) along the different process steps (initial, after gastric and after enteric digestion) are showed in Figs. 5 and 6. The gastric digestion step led to a slight decrease on the zeta potential of uncoated microgels while a significant decrease was observed for the coated microgels. The gellan has a p*K*a value around 3.5 (Mao et al., 1999; Picone & Cunha, 2013), which means that a decrease in the gellan negative charge could be observed when this polysaccharide is poured in a medium with pH lower than 3.5. Concerning to chitosan, a decrease in its positive charge could be observed in pH values above 6.3 (Anal et al., 2008; Picone & Cunha, 2013). Based on the pKa values of gellan and chitosan we can infer that the immersion into the gastric fluid (pH = 2) promoted a decrease of gellan negative charge, promoting a partial displacement of

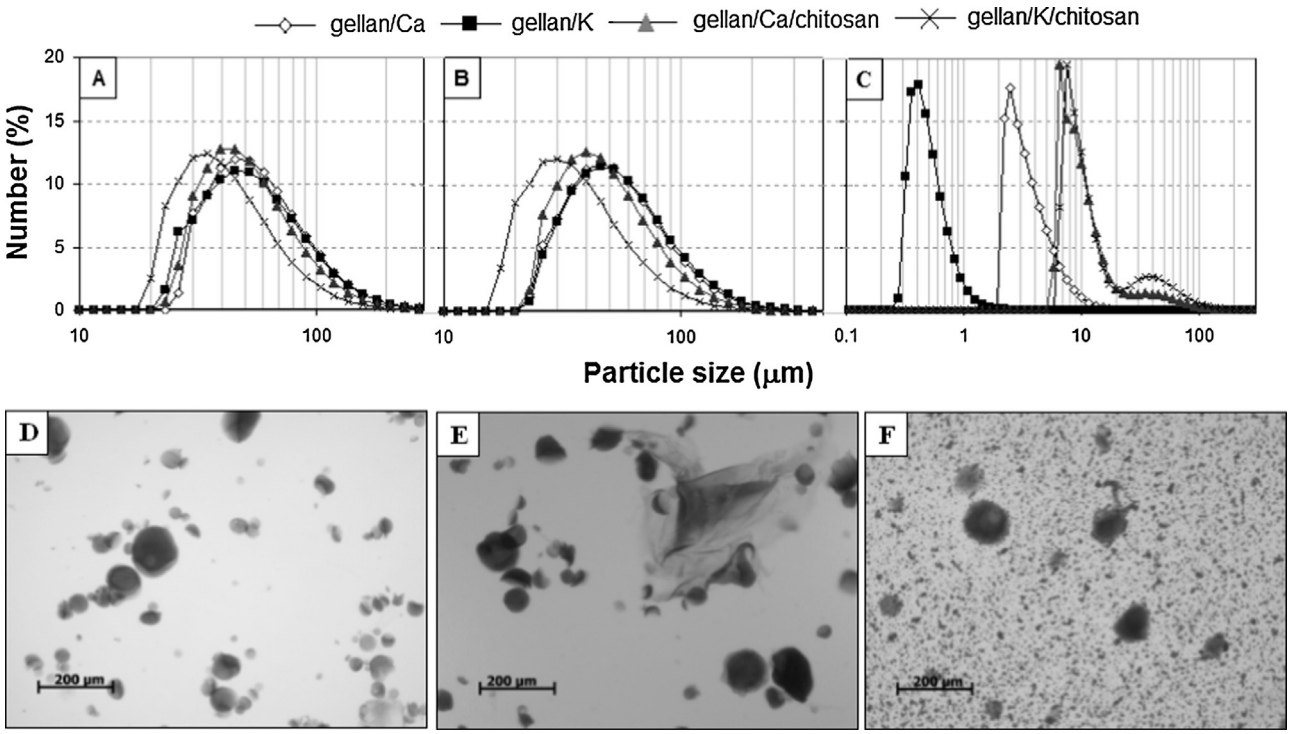

Fig. 6. Particle size distribution at the initial (A), after gastric digestion (B) and after enteric digestion (C). Optical microscopy of gellan/K microgel at initial (D), after gastric digestion (E) and after enteric digestion (F).

chitosan from the coating layer, dissociating partly the gellan-chitosan complexes, explaining the decrease observed for the zeta potential values.

Although the gastric digestion step had showed some effect in the microgels zeta potential, Fig. 6A and B showed that this step did not change significantly the size distribution of the particles. Then all microgels studied could be considered quite resistant to the digestion conditions of the stomach.

The enteric digestion step showed a more pronounced effect on zeta potential of the particles (Fig. 5). The uncoated microgels showed an increase in the magnitude of zeta potential, resulting in high negative values. The gellan/K microgels showed zeta potential values very similar to that found for pure gellan dispersed in water (pure gellan = -44.27 ± 3.71 mV). It could suggest that an almost complete destabilization of the gel network occurred. A hypothesis can be raised to explain this destabilization. It seems that the cations responsible to maintain the gel network were sequestered by ionized bile acids, causing the disruption of the gel (Hur, Lim, Decker, & McClements, 2011). The gellan/Ca microgels showed smaller absolute values of zeta potential, showing that these particles were more resistant to simulated enteric digestion, since the gel network disruption was only partial.

The zeta potential of chitosan-coated microgels changed from positive to negative values after the enteric digestion step. This change is again related to the displacement of the chitosan layer, which was linked to gellan through electrostatic interactions. After the complex dissociation, the carboxylic groups of the gellan chain were again exposed, being responsible for the negative zeta potential values (Anal & Stevens, 2005). The gellan network of the coated-microgels was also partly disrupted after the loss of the chitosan external layer, since the final zeta potential values were close to the values obtained for pure gellan dispersion.

Such gel network disruption suggested by zeta potential values was confirmed by the particle size distribution results (Fig. 6B and C), which shows that a physical fragmentation was observed after the enteric digestion. The microgels were broken into smaller particles, which could also be observed in optical microscopy (Fig. 6E and F) using a representative morphology (gellan/K microgels). Regarding the effect of the enteric digestion step on the coated microgels, two processes could be observed. First, the results suggest that the pH of the simulated enteric juice was responsible by the destabilization of the gellan–chitosan complex, with subsequent sedimentation of insoluble chitosan. After that, we can consider that the particles have been subjected to the same process that occurred with pure gellan microgels, in which the gel disintegration took place.

Although all samples showed structure breakdown after enteric digestion, the particles size distribution (Fig. 6C) indicated a lower fragmentation of the chitosan-coated microgels. This was evidenced by the bimodal size distribution of such samples, in which the second peak (20–100 μm) represents a considerable number of undamaged particles, which was also observed through optical microscopy observation. Therefore, the presence of the outer chitosan layer decreased particle disintegration, delaying the erosion process and thus extending the particle resistance. This delayed disintegration was also observed in alginate beads coated with chitosan (Anal & Stevens, 2005), in which was demonstrated that stronger binding forces in the polyelectrolyte complex matrix increases the time taken for the complete particles disintegration. Concerning to the effect of enteric conditions on the particles studied, in general, the coated-microgels showed greater resistance than the gellan/Ca microgels, which in turn showed lower disintegration degree than gellan/K particles.

4. Conclusions

All microgels, except the gellan/K, showed good stability in aqueous media (pH 6.3 and pH 3). The chitosan coating enhanced the stability of the gellan/K microgels and prevented the disruption of such microgel in aqueous media. The *in vitro* digestion test indicated that the gellan microgels were resistant to the simulated gastric conditions. However, the coated microgels showed a partial displacement of the external layer of chitosan after this digestion step. The subsequent enteric digestion step led to a fragmentation of the microgel structures. Such network disruption was more intense for the uncoated microgels. The additional chitosan layer increased the particles resistance to the enteric conditions, since a significant amount of undamaged particles was observed even after 2 h in the simulated enteric juice. Finally, micrometer-sized particles which could be used as vehicle for bioactive compounds were produced at mild conditions, using a simple process and biocompatible ingredients.

Acknowledgements

The authors are grateful to FAPESP (EMU 09/541371) and CNPq (131179/2010-1) for their financial support. In addition, the authors are grateful for the access allowed to the equipment, and assistance provided by the National Institute of Science and Technology on Photonics Applied to Cell Biology (INFABIC) at the University of Campinas. INFABIC was co-funded by FAPESP (08/57906-3) and CNPq (573913/2008-0).

References

Allen, A., Flemström, G., Garner, A., & Kivilaakso, E. (1993). Gastroduodenal mucosal protection. *Physiological Reviews*, *73*(4), 823–857.

Amaike, M., Senoo, Y., & Yamamoto, H. (1998). Sphere, honeycomb, regularly spaced droplet and fiber structures of polyion complexes of chitosan and gellan. *Macromolecular Rapid Communications*, *19*, 287–289.

Anal, A. K., & Stevens, W. F. (2005). Chitosan–alginate multilayer beads for controlled release of ampicillin. *International Journal of Pharmaceutics*, *290*, 45–54.

Anal, A. K., Tobiassen, A., Flanagan, J., & Singh, H. (2008). Preparation and characterization of nanoparticles formed by chitosan–caseinate interactions. *Colloids and Surfaces B: Biointerfaces*, *64*, 104–110.

Chan, E., Lee, B., Ravindra, P., & Poncelet, D. (2009). Prediction models for shape and size of Ca-alginate macrobeads produced through extrusion-dripping method. *Journal of Colloid and Interface Science*, *338*(1), 63–72.

Colinet, I., Dulong, V., Mocanu, G., Picton, L., & Cerf, D. L. (2010). Effect of chitosan coating on the swelling and controlled release of a poorly water-soluble drug from an amphiphilic and pH-sensitive hydrogel. *International Journal of Biological Macromolecules*, *47*, 120–125.

Cook, M. T., Tzortzis, G., Charalampopoulos, D., & Khutoryanskiy, V. V. (2011). Production and evaluation of dry alginate–chitosan microcapsules as an enteric delivery vehicle for probiotic bacteria. *Biomacromolecules*, *12*, 2834–2840.

Das, M., Zhang, H., & Kumacheva, E. (2006). Microgels: Old materials with new applications. *Annual Review of Materials Research*, *36*, 117–142.

Dash, M., Chiellini, F., Ottenbrite, R. M., & Chiellini, E. (2011). Chitosan—A versatile semi-synthetic polymer in biomedical applications. *Progress in Polymer Science*, *36*, 981–1014.

Delgado, A. V., Gonzalez-Caballero, F., Hunter, R. J., Koopal, L. K., & Lyklema, J. (2005). Measurement and interpretation of electrokinetic phenomena. *Pure and Applied Chemistry*, *77*(10), 1753–1805.

Evageliou, V., Karantoni, M., Mandala, I., & Komaitis, M. (2010). Compression of gellan gels. Part I: Effect of salts. *International Journal of Food Science and Technology*, *45*, 1076–1080.

Garrett, D. A., Failla, M. L., & Sarama, R. J. (1999). Development of an in vitro digestion method to assess carotenoid bioavailability from meals. *Journal of Agricultural and Food Chemistry*, *47*(10), 4301–4309.

Gåserød, O., Jolliffe, I. G., Hampson, F. C., Dettmar, P. W., & Skjåk-Bræk, G. (1998). The enhancement of the bioadhesive properties of calcium alginate gel beads by coating with chitosan. *International Journal of Pharmaceutics*, *175*, 237–246.

Guzey, D., & McClements, D. J. (2006). Formation, stability and properties of multilayer emulsions for application in the food industry. *Advances in Colloid and Interface Science*, *128–130*, 227–248.

Hamman, J. H. (2010). Chitosan based polyelectrolyte complexes as potential carrier materials in drug delivery systems. *Marine Drugs*, *8*, 1305–1322.

Harding, S. E. (2003). Mucoadhesive interactions. *Biochemical Society Transactions*, *31*(5), 1036–1041.

Heilig, A., Göggerle, A., & Hinrichs, J. (2009). Multiphase visualisation of fat containing β-lactoglobulin–κ-carrageenan gels by confocal scanning laser microscopy, using a novel dye, V03-01136, for fat staining. *LWT—Food Science and Technology*, *42*, 646–653.

Herrero, E. P., Del-Valle, E. M. M., & Galán, M. A. (2006). Development of a new technology for the production of microcapsules based in atomization processes. *Chemical Engineering Journal*, *117*, 137–142.

Hoebler, C., Lecannu, G., Belleville, C., Devaux, M. F., Popineau, Y., & Barry, J. L. (2002). Development of an in vitro system simulating bucco-gastric digestion to assess the physical and chemical changes of food. *International Journal of Food Sciences and Nutrition*, *53*, 389–402.

Hur, S. J., Lim, B. O., Decker, E. A., & McClements, D. J. (2011). In vitro human digestion models for food applications. *Food Chemistry*, *125*, 1–12.

Jansson, P., & Lindberg, B. (1983). Structural studies of gellan gum, an extracellular polysaccharide elaborated by *Pseudomonas elodea*. *Carbohydrate Research*, *124*, 135–139.

Kiang, T., Wen, J., Lim, H. W., & Leong, K. W. (2004). The effect of the degree of chitosan deacetylation on the efficiency of gene transfection. *Biomaterials*, *25*, 5293–5301.

Li, M., Rouaud, O., & Poncelet, D. (2008). Microencapsulation by solvent evaporation: State of the art for process engineering approaches. *International Journal of Pharmaceutics*, *363*, 26–39.

Luo, Y., & Wang, Q. (2014). Recent development of chitosan-based polyelectrolyte complexes with natural polysaccharides for drug delivery. *International Journal of Biological Macromolecules*, *64*, 353–367.

Mao, R., Tang, J., & Swanson, B. G. (1999). Effect of pH buffers on mechanical properties of gellan gels. *Journal of Texture Studies*, *30*, 151–166.

Miller, D. D., Schricker, B. R., Rasmussen, R. R., & Van Campen, D. (1981). An *in vitro* method for estimation of iron availability from meals. *American Journal of Clinical Nutrition*, *34*(10), 2248–2256.

Miyoshi, E., Takaya, T., & Nishinari, K. (1996). Rheological and thermal studies of gel–sol transition in gellan gum aqueous solutions. *Carbohydrate Polymers*, *30*, 109–119.

Morris, E. R., Nishinari, K., & Rinaudo, M. (2012). Gelation of gellan—A review. *Food Hydrocolloids*, *28*, 373–411.

Nitta, Y., Ikeda, S., & Nishinari, K. (2006). The reinfocement of gellan gel network by the immersion into salt solution. *International Journal of Biological Macromolecules*, *38*, 145–147.

Norton, A. B., Cox, P. W., & Spyropoulos, F. (2011). Acid gelation of low acyl gellan gum relevant to self-structuring in the human stomach. *Food Hydrocolloids*, *25*, 1105–1111.

Oh, J. K., Lee, D. I., & Park, J. M. (2009). Biopolymer-based microgels/nanogels for drug delivery applications. *Progress in Polymer Science*, *34*(12), 1261–1282.

Ohkawa, K., Kitagawa, T., & Yamamoto, H. (2004). Preparation and characterization of chitosan–gellan hybrid capsules formed by self-assembly at an aqueous solution interface. *Macromolecular Materials and Engineering*, *289*(1), 33–40.

Perrechil, F. A., Vilela, J. A. P., Guerreiro, L. M. R., & Cunha, R. L. (2012). Development of Na-CN–κ-carrageenan microbeads for the encapsulation of lipophilic compounds. *Food Biophysics*, *7*, 264–275.

Perrechil, F. A., Sato, A. C. K., & Cunha, R. L. (2011). κ-Carrageenan–sodium caseinate microgel production by atomization: Critical analysis of the experimental procedure. *Journal of Food Engineering*, *104*, 123–133.

Picone, C. S. F., & Cunha, R. L. (2011). Influence of pH on formation and properties of gellan gels. *Carbohydrate Polymers*, *84*, 662–668.

Picone, C. S. F., & Cunha, R. L. (2013). Chitosan–gellan electrostatic complexes: Influence of preparation conditions and surfactant presence. *Carbohydrate Polymers*, *94*, 695–703.

Poncelet, D., Lencki, R., Beaulieu, C., Halle, J. P., Neufeld, R. J., & Fournier, A. (1992). Production of alginate beads by emulsification/internal gelation. I. Methodology. *Applied Microbiology and Biotechnology*, *38*(1), 39–45.

Ribeiro, A. J., Neufeld, R. J., Arnaud, P., & Chaumeil, J. C. (1999). Microencapsulation of lipophilic drugs in chitosan-coated alginate microspheres. *International Journal of Pharmaceutics*, *187*, 115–123.

Sworn, G., Sanderson, G. R., & Gibson, W. (1995). Gellan gum fluid gels. *Food Hydrocolloids*, *9*(4), 265–271.

Tang, J., Tung, M. A., & Zeng, Y. (1996). Compression strength and deformation of gellan gels formed with mono- and divalent cations. *Carbohydrate Polymers*, *29*, 11–16.

Vilela, J. A. P., Cavallieri, A. L. F., & Cunha, R. L. (2011). The influence of gelation rate on the physical properties/structure of salt-induced gels of soy protein isolate-gellan gum. *Food Hydrocolloids*, *25*, 1710–1718.

Yamamoto, F., & Cunha, R. L. (2007). Acid gelation of gellan: Effect of final pH and heat treatment conditions. *Carbohydrate Polymers*, *68*, 517–527.

Yang, F., Xia, S., Tan, C., & Zhang, X. (2013). Preparation and evaluation of chitosan–calcium–gellan gum beads for controlled release of protein. *European Food Research and Technology*, *237*, 467–479.

Zhang, L., & Kosaraju, S. L. (2007). Biopolymeric delivery system for controlled release of polyphenolic antioxidants. *European Polymer Journal*, *43*, 2956–2966.

Zou, Q., Zhao, J., Liu, X., Tian, F., Zhang, H., Zhang, H., et al. (2011). Microencapsulation of Bifidobacterium bifidum F-35 in reinforced alginate microspheres prepared by emulsification/internal gelation. *International Journal of Food Science and Technology*, *46*, 1672–1678.